Ocean Engineering 153 (2018) 345–352

Contents lists available at ScienceDirect

Ocean Engineering

journal homepage: www.elsevier.com/locate/oceaneng

Hydrodynamic loads on a circular cylinder surrounded by two, four and eight wake-control cylinders

M. Silva-Ortega [1], G.R.S. Assi [*]

Department of Naval Architecture & Ocean Engineering, Escola Politécnica, University of São Paulo, São Paulo, Brazil

A R T I C L E I N F O

Keywords:
Vortex shedding
Wake control
Drag reduction
Axial rods
Shrouds

A B S T R A C T

The hydrodynamic loads of mean drag and fluctuating lift are presented for a circular cylinder fitted with 2, 4 and 8 wake-control cylinders positioned around its circumference. The device is fitted around the body to interact with the flow in the near wake and control vortex shedding. The efficiency regarding lift suppression and drag reduction has been investigated for nine different cases varying the diameter of the control cylinders and their relative gap from the wall. All cases have been compared with the hydrodynamic forces of a plain cylinder. The configuration with 4 control cylinders, gap ratio of $G/D = 0.05$ (G is the gap between the control cylinders and the main cylinder of diameter D) and diameter ratio of $d/D = 0.06$ (d is the diameter of the control cylinders) produced the lowest drag when compared to all other configurations: mean drag coefficient was 0.75, approximately 50% lower than that of a bare cylinder. Experiments have been conducted in a free-surface water channel at moderated Reynolds numbers between 5000 and 50,000.

1. Introduction

The periodic shedding of vortices downstream of a bluff body generates cyclic hydrodynamic loads that feed back on the body. Fluctuating lift will be at the frequency (f_s) in which vortices are shed in the wake, while drag will be at double that frequency ($2f_s$). With time, the cyclic loads may cause structural problems to the body, such as fatigue damage, a special concern for slender structures as riser pipes and submarine cables. Flexible structures with a bluff shape may be excited by this periodic load and respond with considerable oscillations. The motion of the structure interacts with the flow and develop into what is called vortex-induced vibrations (VIV).

Mitigating vortex shedding and VIV are important issues for many engineering applications, ranging from aeroacoustic problems in aviation to the vibration of a drilling riser in offshore exploration. Hence, the scientific community and the industry are constantly pursuing the development of new methods to control the wake and design novel VIV suppressors (devices attached to the body to mitigate the damaging effects of the vibration).

Wake-control mechanisms can be classified as passive or active systems (Choi et al., 2008), with the latter considering both open-loop and closed-loop control systems. Zdravkovich (1981) presents several passive-control devices, classifying them into three categories according to the way they affect the vortex-shedding mechanism: (i) Surface protrusions, which affect separation lines and/or separated shear layers: they involve helical strakes, wires, fins, studs, or spheres, among others. (ii) Shrouds, that affect the entrainment layers around the body. The perforated shroud and the axial rods are two examples. (iii) Near-wake stabilizers, that affect the switch of the confluence point. Fairings and splitter plates, which prevents communication between the opposing shear layers of the wake, are common examples. These passive methods require no external energy supply and they act primarily disrupting the formation and development of an organized wake of vortices.

Among the various solutions for passive vortex-shedding and VIV suppression, the helical strakes are one of the most commonly used in air and water flows (Bearman and Brankovic, 2004; Korkischko and Meneghini, 2010). But despite the proven efficiency of the strakes in reducing fluctuating lift, they increase the mean drag (Korkischko and Meneghini, 2011; Zdravkovich, 1981), which is undesirable in a great number of applications.

Placing a smaller control rod upstream of the main cylinder is a well-established strategy for drag reduction (Lee et al., 2004). Strykowski and Sreenivasan (1990) proved that if the small control cylinder is otherwise placed within a defined region in the near-wake (downstream) of the main cylinder, the wake could be effectively suppressed at a Reynolds number of $Re = 80$. Suppression of the vortex street is associated with

* Corresponding author.
E-mail address: g.assi@usp.br (G.R.S. Assi).
[1] Currently at Department of Naval Engineering, University Veracruzana, Mexico.

https://doi.org/10.1016/j.oceaneng.2018.01.116
Received 7 October 2016; Received in revised form 29 January 2018; Accepted 31 January 2018
Available online 20 February 2018

damping the instability in the near-wake region. In their investigation, the ratio between the diameter of the control cylinder to the diameter of the main cylinder varied between $d/D = 1/3$ to $1/20$. They also showed that wake suppression is the most efficient when the small control cylinder is placed roughly around $1D$ downstream of the cylinder center and $1D$ to the side of the centerline of the wake for $d/D = 0.05$ to 0.07. Their experimental and numerical results also indicate that this region of effectiveness strongly depends on Re and d/D. For $Re = 80$ to 300, Kuo et al. (2007) showed detailed flow structures revealing the primary mechanism that led to significant lift and drag reduction without completely suppressing the shedding of a vortex street.

Zdravkovich (1981) presented results of an axial-rod shroud, following the concept that the shroud should break-up the flow into a large number of small vortices. Axial rods were fitted about the circular cylinder and several parameters were varied in order to find an optimum configuration for VIV suppression: the number of rods (varied between 4 and 218, defining the shroud porosity), the distance of the rods to the wall of the cylinder (gap) and their circumferential distribution. Tests were performed in a water channel and in a wind tunnel for $Re \approx 10^3$–10^5. The most interesting result, as far as suppression was concerned, was obtained for a porosity of 63% (39 rods) when the rods were positioned with a gap of $G/D \approx 0.25$ from the cylinder wall. But most surprisingly was the fact that the best suppression was achieve when the rods were not evenly distributed around the cylinder, but grouped close to the near wake, leaving an unshrouded portion (of about 90 degrees of the circumference) facing the free stream.

More recently, control of the wake of a cylinder with rotating control cylinders has been investigated experimentally (Korkischko and Meneghini, 2012) and numerically (Mittal, 2001; Silva-Ortega et al., 2014b). In a recent study, Silva-Ortega and Assi (2017) reported on VIV experiments performed with the same control cylinder discussed in the present work acting as VIV suppressors. They found that the best VIV suppressor was "composed of 8 control cylinders and mitigated 99% of the peak amplitude of vibration when compared to that of a plain cylinder; mean drag was increased by 12%". They also concluded that "a polar array of 4 control cylinders was the most efficient configuration to minimize the mean drag, but the system developed severe vibrations combining VIV and a galloping-like response".

The objective of the present work is to investigate a method of suppressing the vortex wake of a circular cylinder employing a passive control strategy. A rigid section of a circular cylinder of diameter D is surrounded by a polar array of $N = 2$, 4 and 8 smaller control cylinders of diameter d, equally spaced about the circumference and separated by a gap G from the wall of the main cylinder. The ratios d/D and G/D are the control parameters of the experimental investigation. As seen above, previous results found in the literature indicate that there are many other significant parameters apart from the number and size of the control cylinders. Therefore, we have conducted an experimental investigation trying to probe the domain of only a few of those governing parameters.

The diameter of the control cylinders (d) was varied in three steps around the size of the smaller cylinders reported by Strykowski and Sreenivasan (1990). Since the vortex-formation length tends to be reduced by an increase in Re, the region of effective wake control presented by Strykowski and Sreenivasan (1990) for $Re = 80$ should be brought much closer to the base of the cylinder for our Re range. Inspired by the work of Zdravkovich (1981), the gap between the control cylinders and the wall of the main cylinder (G) was also varied in three steps. In the present parametric study neither the main cylinder nor the control cylinders were allowed to move or respond to the flow, so the efficiency of the wake-control method was evaluated by measuring the hydrodynamic loads acting on the body.

2. Experimental method

Experiments have been carried out in the recirculating water channel of NDF (Fluids and Dynamics Research Group) at the University of São Paulo, Brazil. The water channel has a free-surface test section which is 0.7 m wide, 0.9 m deep and 7.5 m long. Good quality flow can be achieved up to 1.0 m/s with turbulence intensity less than 3%. This laboratory has been especially designed for experiments with flow-induced vibrations. For further details the apparatus, validation and information on the facilities please refer to Assi et al. (2013, 2010a, 2010b).

A rigid section of a circular cylinder was made of a perspex tube of external diameter $D = 100$mm with a smooth surface. Two, four or eight identical control cylinders were made of perspex rods and supported by rings attached to the ends of the main cylinder. The distribution of the control cylinders about the main cylinder is presented in Fig. 1, in which the arrow indicates the direction of the incoming flow. The position of the N control cylinders was chosen so that they were equally spaced around the main cylinder, but keeping a symmetric distribution in relation to the streamwise axis, with no cylinder at the frontal stagnation point.

The axes of the control cylinders were parallel to the axis of the main cylinder, spanning the whole length of the model (immersed length of $L = 700$mm). Two extra supporting rings were installed at $L/3$ and $L2/3$ positions to hold the control cylinders in place and prevent them from vibrating by reducing their free span. The control cylinders did not present significant deflections nor vibrations due to their own VIV in the course of the experiments. The diameter of the control cylinders was varied in three steps of $d/D = 0.04$, 0.06 and 0.08. The gap measured between the wall of the control cylinders and the wall of the main cylinder could be set to $G/D = 0.05$, 0.10 and 0.15. The angular distribution of the control cylinders was kept constant for all cases while varying d/D and G/D. The models were the same employed by Silva-Ortega and Assi (2017).

Models were mounted on a especially built load cell (developed by Assi, 2009), rigidly attached to the frame of the test section to deduce the instantaneous and time-averaged hydrodynamic forces on the cylinder model. An illustration of the experimental setup is presented in Fig. 2. A summary of all the parameters investigated in the experiment is presented in Table 1, adding up to 27 different experimental configurations. In addition, preliminary tests have been performed with a bare cylinder (without control cylinders) to serve as a reference for comparison. The only flow variable changed during the course of the experiments was the flow velocity U, which alters the Reynolds number ($Re = UD/\nu$, based on the diameter D of the bare cylinder and the viscosity of water ν) between 5000 and 50,000.

3. Results

Measurements of lift and drag were made for each of the 27 configurations presented above. Results for a bare cylinder in the range $Re = 5,000$ to 50,000 are presented as a reference and for validation. This Re range falls in the subcritical regime in which transition to turbulence occurs in the separated shear layers and a considerable scatter of lift and drag is found in the literature (Zdravkovich, 1997). The mean drag coefficient ($\overline{C}_D$) and the RMS of the lift coefficient ($\widehat{C}_L$) are presented for a bare (or plain) cylinder in Fig. 3. In Fig. 3a, mean drag for the plain cylinder remains roughly around $\overline{C}_D \approx 1.4$, not too far but higher than the curve presented by Zdravkovich (1997), who summarized results from various sources.

It is worth highlighting that, in the present experiments, the top end of the cylinder pierced the free surface of the water, hence a small fraction of the drag is due to the generation of waves. The Froude number ($Fr = U/\sqrt{gD}$, where g is the acceleration of gravity) was rather small, varying between $Fr = 0.05$ and 0.5 for a constant ratio of Reynolds number to Froude number of $Re/Fr \approx 10^5$. Chaplin and Teigen (2003), who measured the wave-resistance drag on a bare cylinder piercing a free surface at $Re/Fr = 2.79 \times 10^5$, concluded that an increase in drag due to the formation of waves is only significant for Fr around 1 and should not

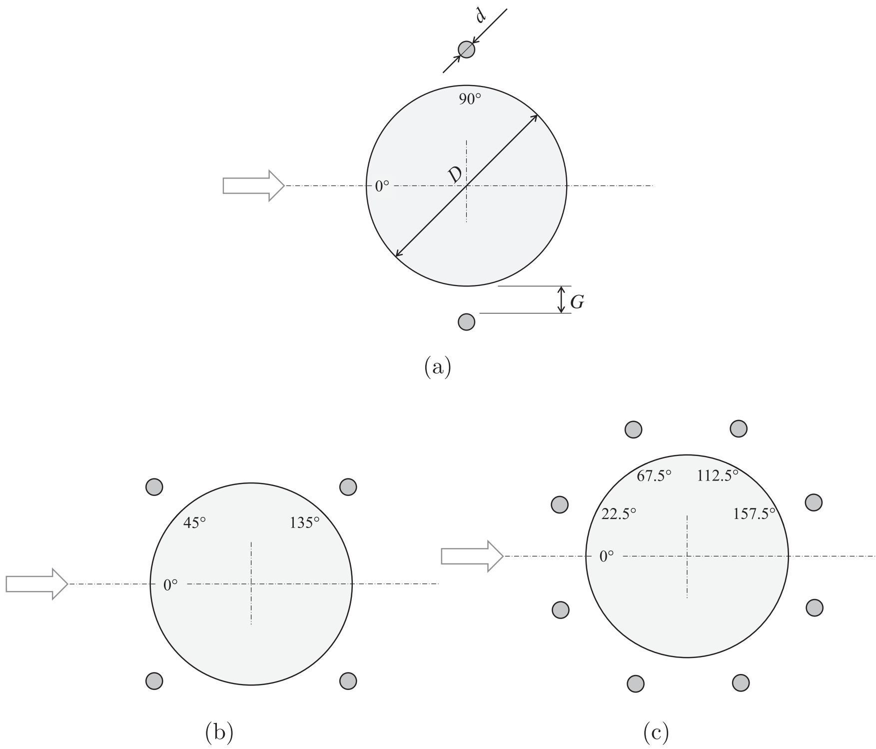

Fig. 1. Geometrical parameters for the main cylinder with (a) two, (b) four and (c) eight control cylinders. Flow approaching in the direction of the arrow.

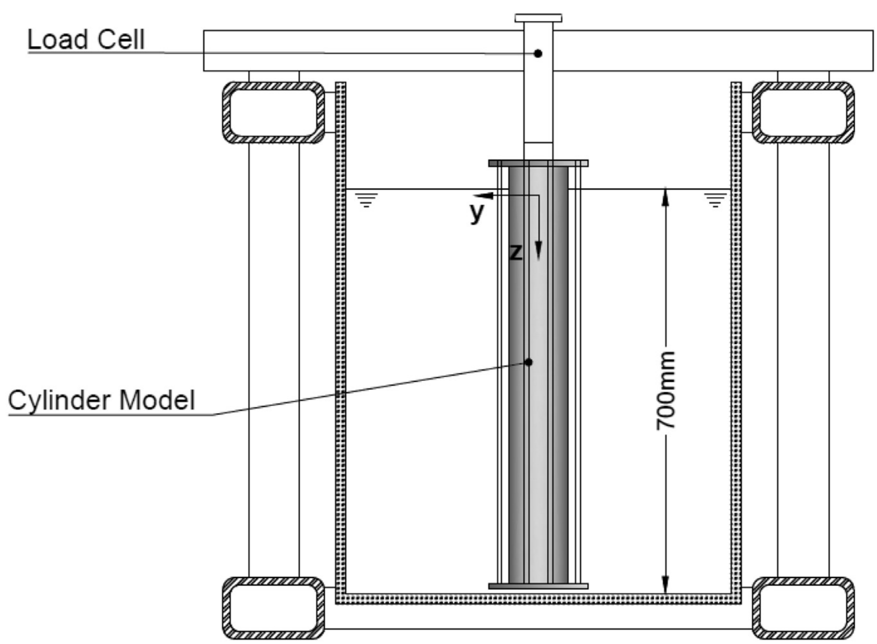

Fig. 2. Experimental setup: cylinder control cylinders mounted on the load cell.

Table 1
Parameters for the present investigation.

Number of control cylinders	N	0, 2, 4, 8
Diameter ratio of the control cylinders	d/D	0.04, 0.06, 0.08
Gap ratio between cylinders	G/D	0.05, 0.10, 0.15
Reynolds number	Re	5×10^3 to 5×10^4
Froude number	Fr	5×10^{-2} to 5×10^{-1}

occur for the $Fr < 0.5$, which is the case in the present experiments. Other effects, due to free stream turbulence intensity (Bell, 1983) or cylinder aspect ratio (Zdravkovich et al., 1989), for example, may contribute to change the mean drag from the canonical value expected for a two-dimensional body. Nevertheless, since all models have been measured under the same condition, the current value of $\overline{C}_D$ for a plain cylinder will be taken as a reference for comparison in this study.

Fig. 3b compares the RMS of lift to the data collected by Norberg (2003). In our study, the overall force acting on the cylinder was measured with a load cell positioned on the top. Due to three-dimensional flow effects, $\widehat{C}_L \approx 0.3$ differs from that expected for a two-dimensional section of the cylinder. Norberg (2003) analyzed several experimental and numerical results at different conditions and

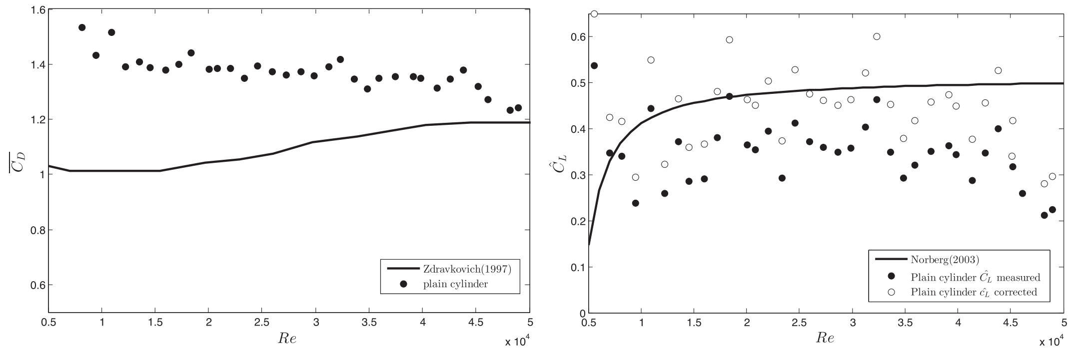

(a) (b)

Fig. 3. (a) Mean drag coefficient and (b) RMS of lift coefficient versus *Re* for the bare cylinder. Results compared to Zdravkovich (1997) and Norberg (2003).

proposed an expression to convert three-dimensional lift ($\hat{c}_L$) into sectional lift ($\hat{c}_L$), taking into account *Re* and the aspect ratio of the body. Therefore, Fig. 3b also presents the corrected $\hat{c}_L \approx 0.4$, as proposed by Norberg (2003), which is in good agreement with the results collected in the literature.

Tests with $N = 2$, 4 and 8 control cylinders with different diameters (d/D), were performed for the same *Re* range of the bare cylinder. For each configuration, $\overline{C}_D$ and $\hat{C}_L$ were measured for 36 equally spaced values of *Re* as flow speed was increased. In order to evaluate the force coefficients, the cylinder diameter (D), was employed as a standard dimension for all configurations. It is known that the effective external diameter of the system is slightly different depending on the distribution, diameter and gap of the control cylinders for each case. Silva-Ortega and Assi (2017) suggested the use of the combined parameter $(G+d)/D$, simply representing the "outermost radial distance of the control cylinders from the wall of the main cylinder, in a way suggesting how far into the flow the control cylinders could interfere." In the present study, $(G+d)/D$ varied between 0.09 and 0.23. However, as far as hydrodynamic forces are concerned, the frontal area of the model did not change as G was increased for each d. Also, variations in d only slightly changed the frontal area. Therefore, we believe the main body's diameter (D) is the most representative dimension to non-dimensionalize the hydrodynamic loads so that they could be compared against each other for each case.

Results are presented in three sets, grouped by the diameter of the control cylinders.

3.1. Control cylinders with $d/D = 0.04$

$\overline{C}_D$ for all cases with $d/D = 0.04$ is shown in Fig. 4a. Apart from the lowest values of *Re*, the behavior of each case is quite clear. All cases with 2 control cylinders (2 cyl.) presented $\overline{C}_D$ higher than that of the bare cylinder, with the case $G/D = 0.15$ showing the highest $\overline{C}_D \approx 1.8$. The cases with 4 control cylinders (4 cyl.) presented the highest variations, with the great majority of points falling below $\overline{C}_D$ for the bare cylinder. The case $G/D = 0.05$, in special, presented the lowest $\overline{C}_D \approx 0.8$ of all cases for most of the *Re* range. All cases with 8 control cylinders (8 cyl.) presented values below $\overline{C}_D$ for the bare cylinder; also showing the smaller dispersion within the group.

Fig. 4b shows $\hat{C}_L$ for all cases with $d/D = 0.04$. Like before, all cases with 2 control cylinders tend to show $\hat{C}_L$ higher than that of the bare cylinder. Cases with 4 control cylinders tend to show $\hat{C}_L$ below the value for the bare cylinder. But more importantly, cases with 8 control cylinders showed the lowest values of $\hat{C}_L$ for the *Re* range, with the cases $G/D = 0.05$ and 0.10 presenting the RMS of lift very close to zero.

(Please note that the limits of the vertical axes in all figures were kept the same to allow for direct qualitative comparison between all figures in the paper.)

3.2. Control cylinders with $d/D = 0.06$

Fig. 5a shows $\overline{C}_D$ for all cases with $d/D = 0.06$. At first sight, one may realize that the larger diameter of the control cylinders has increased $\overline{C}_D$ for all cases. For most cases this might be due to the increase of the effective diameter of the body. While all cases with 2 control cylinders produced the highest $\overline{C}_D$, all cases with 8 control cylinders now fall in the middle, but still with $\overline{C}_D$ below that for the bare cylinder. With the lowest $\overline{C}_D$, now appears the group with 4 control cylinders, with the case $G/D = 0.05$ showing the lowest $\overline{C}_D \approx 0.75$ for most of the *Re* range.

Results of $\hat{C}_L$ in Fig. 5b are not very different. All cases with 2 control cylinders produce the highest RMS of lift, above the value for the bare cylinder. On the other hand, all cases with 4 and 8 control cylinders managed to reduce $\hat{C}_L$ below that of a bare cylinder for most of the *Re* range, highlighting cases 8 cyl. with $G/D = 0.15$ and 4 cyl. with $G/D = 0.05$ that produced almost zero $\hat{C}_L$.

3.3. Control cylinders with $d/D = 0.08$

Finally, Fig. 6a presents $\overline{C}_D$ for cases with $d/D = 0.08$. With the largest control cylinders, almost all cases presented $\overline{C}_D$ roughly equal or higher than that of the bare cylinder. The exception was the group with 4 control cylinders, which showed $\overline{C}_D \approx 1$ for most of the *Re* range. This time, the cases with 4 control cylinders and $G/D = 0.05$ and 0.10 presented the lowest $\overline{C}_D$.

The RMS of lift shown in Fig. 6b follows the same behavior seen before, with all cases with 2 control cylinders showing higher $\hat{C}_L$ than that of the bare cylinder. Again, cases with 4 and 8 control cylinders reduced $\hat{C}_L$ considerably, with cases $N = 8$ with $G/D = 0.10$ and $N = 4$ with $G/D = 0.05$ reaching almost zero $\hat{C}_L$.

4. Discussion

It is easy to get confused with so many response curves considering the variations in all three parameters: N, d/D and G/D. The first general consideration to be made is that the position of the control cylinders in relation to the flow is indeed very important. The three parameters combined work to alter the influence of the control cylinders over the near wake, not to mention their influence over the flow before it separates from the body.

For example, for the case with $N = 2$, it is believed that the control cylinders are interfering with the flow near the separation points, since they are positioned at $\pm 90°$ in relation to the incoming flow. With 4 control cylinders, we can still suppose that the rear cylinders (located at

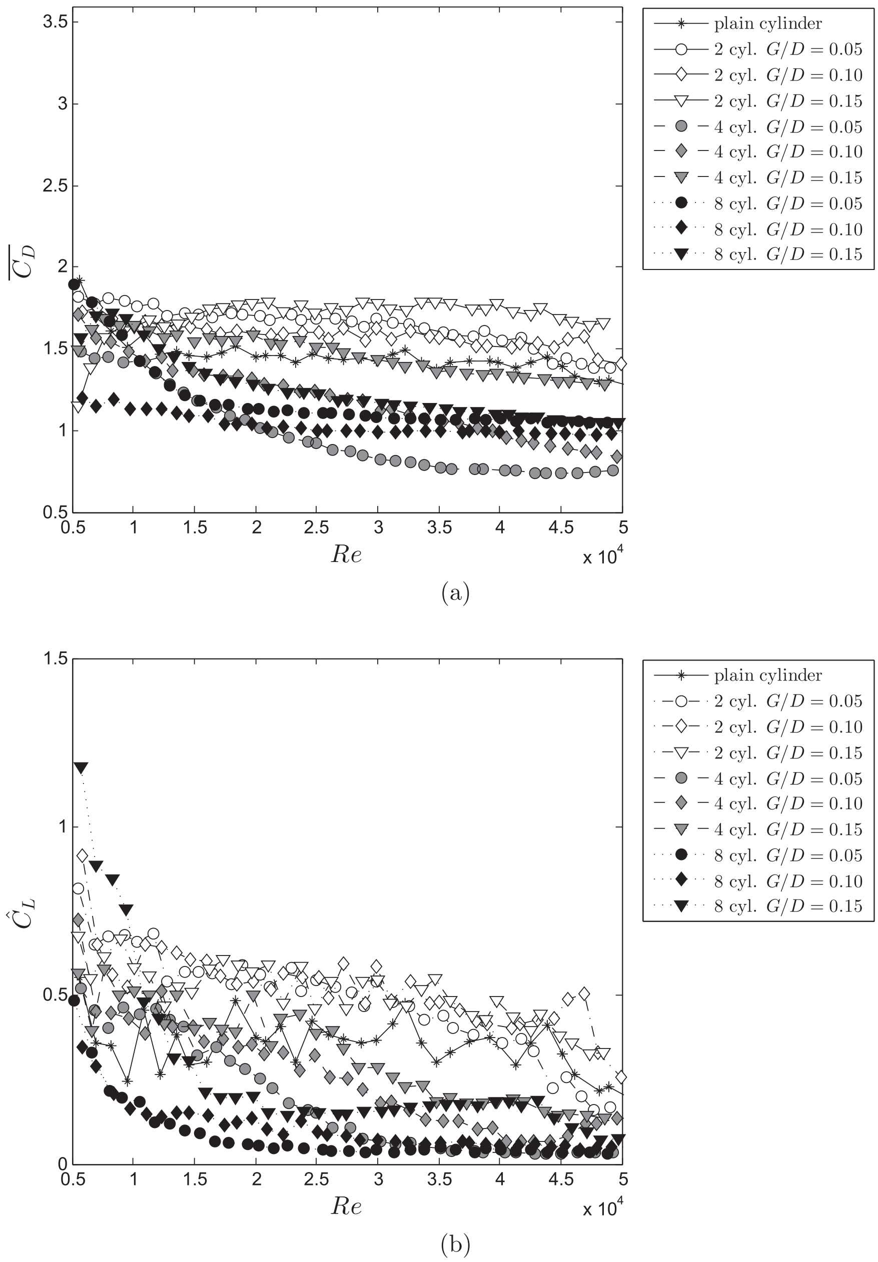

Fig. 4. (a) Mean drag coefficient and (b) RMS of lift versus *Re* for 2, 4 and 8 control cylinders with $d/D = 0.04$ and varying gap.

$\pm 135^{\circ}$) interact with the separating flow and/or the separated shear layers in the near wake, but the front cylinders (located at $\pm 45^{\circ}$) are most likely interacting with the attached boundary layers. The same must be happening with $N = 8$: while cylinders positioned at $\pm 22.5^{\circ}$ and $\pm 67.5^{\circ}$ are most likely interacting with the boundary layer, cylinders at $\pm 112.5^{\circ}$ are located very near the natural separation points, while cylinders at $\pm 157.5^{\circ}$ might be interacting with the near wake. This is supported by the flow visualization provided by the numerical simulations performed by Silva-Ortega et al. (2014a,b) at $Re = 100$.

The cases with 2 control cylinders have shown a behavior similar to that observed by Mittal (2001), who performed numerical simulation of the flow past a circular cylinder at $Re = 10^4$, with $d/D = 0.05$ and $G/D = 0.075$. In their case, the numerical simulations allowed for a better understanding of the flow. In our study, among all experiments, the cases with $N = 2$ consistently appeared as the worst arrangement to suppress $\widehat{C}_L$ and reduce $\overline{C}_D$. It actually increased drag above the value for a bare cylinder. On the other hand, the cases with 4 control cylinders with diameters $d/D = 0.06$ and 0.08 presented a considerable reduction of $\widehat{C}_L$ with the lowest $\overline{C}_D$.

Recently, motivated by the work of Strykowski and Sreenivasan (1990), Patino et al. (2015) performed flow sensibility analysis of the flow to study the effects of wake control with small cylinders located around the main cylinder with $d/D = 0.06$ and $G/D = 0.07$ at $Re = 47$. Changing the position of a single control cylinder around the main cylinder, they found that the wake became stable when the control cylinder was positioned at 0°–50°, 135°–225° and 310°–360°, thus inhibiting the formation of vortices. Please note that their study suggested an effective control of the wake with control cylinder positioned at the front and at the back of the main body.

Of course the sensibility analysis conducted by Patino et al. (2015) was focusing at an extremely low *Re*, at the beginning of the hydrodynamic instability that leads to the formation of the vortex wake. Nevertheless, leaving the difference of *Re* aside, we cannot ignore the fact that, in our work, only the cases with $N = 4$ and 8 have cylinders located within the regions highlighted by Patino et al. (2015). Those cases were precisely the ones to present the most reduction in $\widehat{C}_L$ and $\overline{C}_D$. It is worth

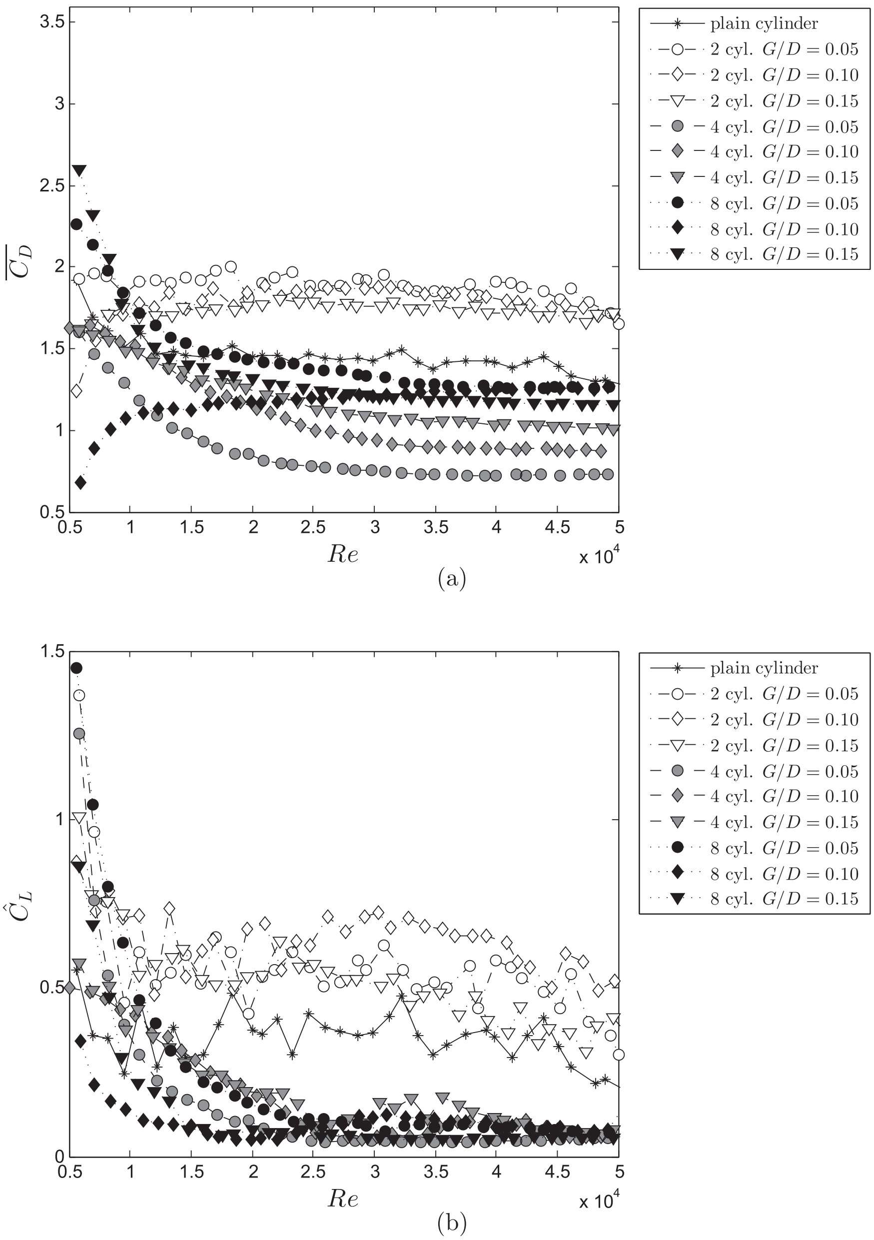

Fig. 5. (a) Mean drag coefficient and (b) RMS of lift versus *Re* for 2, 4 and 8 control cylinders with $d/D = 0.06$ and varying gap.

noting that the case with 8 control cylinders is the closest to an omnidirectional system tested in this investigation, even though with discrete elements positioned 45° apart. Needless to say that an omnidirectional device would be very interesting for practical applications in engineering.

Finally, considering only the diameters of the control cylinders, cases with $d/D = 0.06$ have shown a slight advantage in reducing $\widehat{C}_L$ and $\overline{C}_D$ over the other cases. Interestingly, $d/D = 0.06$ was not the smallest nor the largest of the tested diameters. Finally the G/D parameter showed the lowest influence on the results when compared to the effect of d/D and N. All this could tell us that there is an optimum value of d/D to suppress the wake and it would probably be dependent on *Re*, the distribution of control cylinders and weakly dependent on G/D (within the range of this investigation).

The current investigation does not provide information on the hydrodynamic interaction of the bodies, only presented the hydrodynamic loads experienced by the cylinder. Future studies should investigate the flow to look for the physical mechanisms in action. It is widely accepted that if the wake is controlled and the shedding of vortices is eliminated the bluff body will not only generate considerably less drag but will also become invulnerable to vortex-induced vibrations.

5. Conclusion

We have presented the hydrodynamic loads of mean drag ($\overline{C}_D$) and fluctuating lift ($\widehat{C}_L$) for a circular cylinder fitted with $N = 2$, 4 and 8 control cylinders positioned around its circumference. The efficiency regarding the mitigation of $\widehat{C}_L$ and reduction of $\overline{C}_D$ was investigated for 27 different cases varying the diameter of the control cylinders (d/D) and their relative distance from the wall G/D). All cases have been compared with the hydrodynamic forces of a plain cylinder.

Cases with $N = 4$ and 8 appeared to perform much better than the cases with 2 control cylinders. This might not be directly related to the total number of control cylinders (N), but instead with the actual position of the cylinder around the main body. Having learnt from previous investigations (Strykowski and Sreenivasan, 1990; Patino et al., 2015), we believe the position of the control cylinders is crucial to the way they interfere with the flow to control the wake. For a future optimization

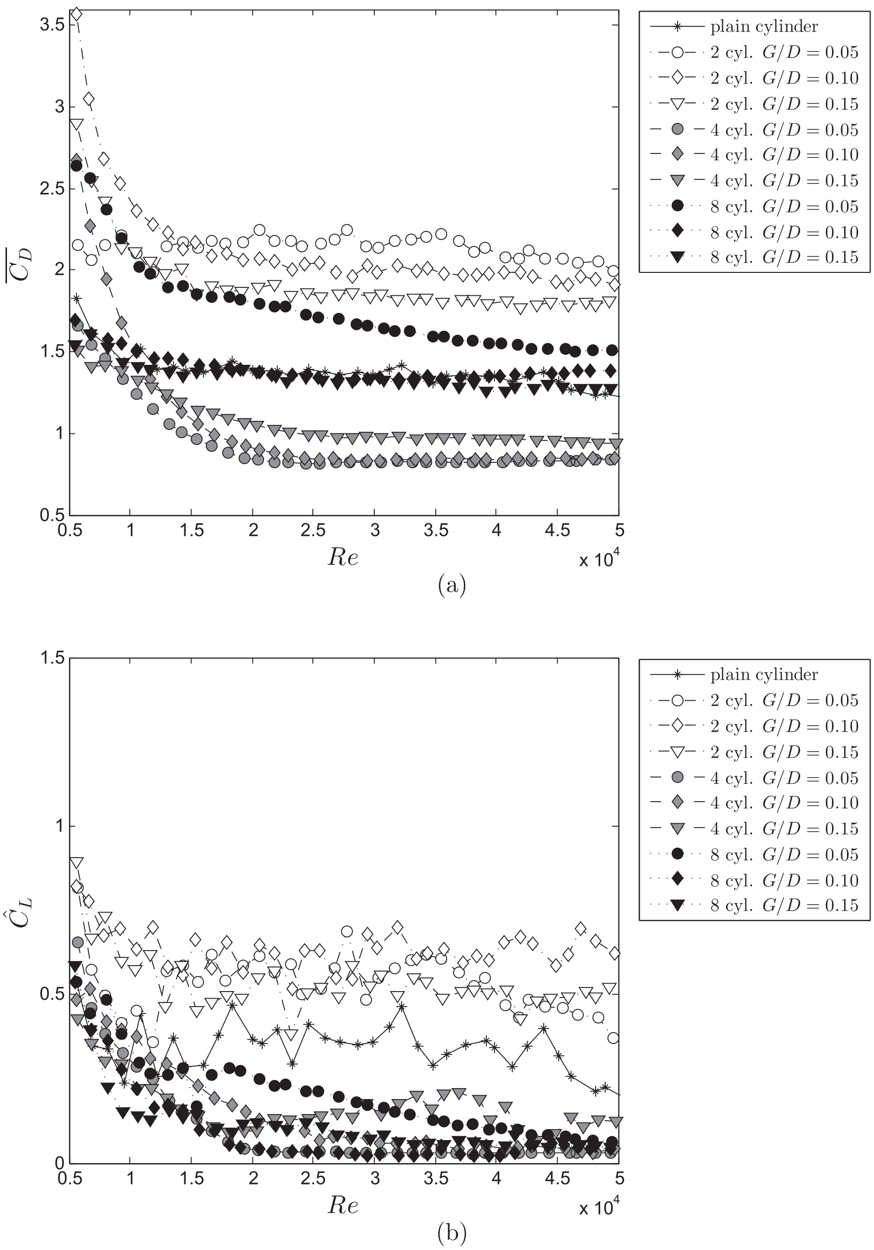

Fig. 6. (a) Mean drag coefficient and (b) RMS of lift versus *Re* for 2, 4 and 8 control cylinders with $d/D = 0.08$ and varying gap.

study, the angular distribution of the control cylinders must be investigated with a much smaller step than the one we have employed in this work (especially when compared with the small variations performed in the d/D and G/D parameters).

The configuration with 4 control cylinders with $G/D = 0.05$ and $d/D = 0.06$ produced the lowest drag when compared to all other configurations: $\overline{C}_D \approx 0.75$, approximately 50% lower than that of a bare cylinder. For the configuration with 8 control cylinders with $d/D = 0.04$, all G/D ratios showed an average $\overline{C}_D \approx 1$, which corresponds to a 33% reduction. Only the configurations with 2 control cylinders showed a 10% increase in drag, with $\overline{C}_D \approx 1.66$ on average.

There is no guarantee that a fixed cylinder with low $\widehat{C}_L$ will not oscillate due to VIV once it is free to respond, especially if a low mass-damping system is concerned. However, a suppressor that produces low $\widehat{C}_L$ in a fixed condition might produce a system with low VIV response, if not get VIV suppressed altogether. Not coincidentally, the case with $N = 8$, $d/D = 0.08$ and $G/D = 0.10$ that presented one of the lowest $\widehat{C}_L$ in the present work, was also the most successful in suppressing VIV in the work of Silva-Ortega and Assi (2017). Future work in this topic will also consider the rotation of the control cylinders, as we explore active-control methods.

Finally, the wave interaction between the control cylinders and the main cylinder produced rather interesting patterns that sometimes appeared to increase and other times to reduce the height of the waves being formed. The wave interaction between the various configurations of control cylinders and its effect on drag or VIV were not properly understood. Based on the principle that there might be an arrangement of control cylinders to suppress the formation of a vortex wake, it is possible that an arrangement of interacting control cylinder could be able to mitigate the formation of surface waves. This questions certainly appears as an interesting topic for future research.

Acknowledgments

MSO is grateful to CAPES Brazilian Ministry of Education. GRSA acknowledges the support of FAPESP (2011/00205-6, 2014/50279-4), CNPq (306917/2015-7) and the Brazilian Navy.

References

Assi, G., Bearman, P., Kitney, N., Tognarelli, M., 2010a. Suppression of wake-induced vibration of tandem cylinders with free-to-rotate control plates. J. Fluid Struct. 26, 1045–1057.
Assi, G.R.S., 2009. Mechanisms for flow-induced vibration of interfering bluff bodies. Phd thesis. Imperial College London.
Assi, G.R.S., Bearman, P.W., Carmo, B.S., Meneghini, J.R., Sherwin, S.J., Willden, R.H.J., 2013. The role of wake stiffness on the wake-induced vibration of the downstream cylinder of a tandem pair, 3 J. Fluid Mech. 718, 210–245.
Assi, G.R.S., Bearman, P.W., Meneghini, J.R., 2010b. On the wake-induced vibration of tandem circular cylinders: the vortex interaction excitation mechanism, 10 J. Fluid Mech. 661, 365–401.
Bearman, P.W., Brankovic, M., 2004. Experimental studies of passive control of vortex-induced vibration. Eur. J. Mech. B Fluid 23, 9–15.
Bell, W., 1983. Turbulence vs drag—some further considerations. Ocean Eng. 10 (1), 47–63.
Chaplin, J., Teigen, P., 2003. Steady flow past a vertical surface-piercing circular cylinder. J. Fluid Struct. 18 (3), 271–285.
Choi, H., Jeon, W.-P., Kim, J., 2008. Control of flow over a bluff body. Annu. Rev. Fluid Mech. 40, 113–139.
Korkischko, I., Meneghini, J.R., 2010. Experimental investigation of flow-induced vibration on isolated and tandem circular cylinders fitted with strakes. J. Fluid Struct. 26 (4), 611–625.
Korkischko, I., Meneghini, J.R., 2011. Volumetric reconstruction of the mean flow around circular cylinders fitted with strakes. Exp. Fluid 51, 1109–1122.
Korkischko, I., Meneghini, J.R., 2012. Suppression of vortex-induced vibration using moving surface boundary-layer control. J. Fluid Struct. 34, 259–270.
Kuo, C.-H., Chiou, L.-C., Chen, C.-C., 2007. Wake flow pattern modified by small control cylinders at low Reynolds number. J. Fluid Struct. 23, 938–956.
Lee, S.-J., Lee, S.-I., Park, C.-W., 2004. Reducing the drag on a circular cylinder by upstream installation of a small control rod. Fluid Dynam. Res. 34 (4), 233–250.
Mittal, S., 2001. Control of flow past bluff bodies using rotating control cylinders. J. Fluid Struct. 15 (2), 291–326.
Norberg, C., 2003. Fluctuating lift on a circular cylinder: review and new measurements. J. Fluid Struct. 17, 57–96.
Patino, G., Silva-Ortega, M., Gioria, R.S., Assi, G.R.S., Meneghini, J.R., 2015. Investigation of circular-cylinder VIV passive-control device using flow sensitivity analysis. In: Bifurcations and Instabilities in Fluid Dynamics. BIFD2015, France.
Silva-Ortega, M., Assi, G., 2017. Flow-induced vibration of a circular cylinder surrounded by two, four and eight wake-control cylinders. Exp. Therm. Fluid Sci. 85, 354–362.
Silva-Ortega, M., Orselli, R.M., Assi, G., 2014a. Control of rotating cylinders as suppressors of vortex-induced vibration of a bluff body. In: Proceedings of SOBENA2014 the 25th Congress of the Brazilian Society of Naval Architects. SOBENA.
Silva-Ortega, M., Orselli, R.M., Assi, G., 2014b. Control of vortex shedding of a circular cylinder with two and four small rotating cylinders. In: Proceedings of EPTT2014 the XI Spring School of Turbulence and Transition. ABCM.
Strykowski, P.J., Sreenivasan, K.R., 1990. On the formation and suppression of vortex shedding at low Reynolds numbers. J. Fluid Mech. 218, 71–107.
Zdravkovich, M., 1981. Review and classification of various aerodynamic and hydrodynamic means for suppressing vortex shedding. J. Wind Eng. Ind. Aerod. 7, 145–189.
Zdravkovich, M.M., 1997. Flow Around Circular Cylinders: Fundamentals, vol. 1. Oxford University Press, New York.
Zdravkovich, M.M., Brand, V.P., Mathew, G., Weston, A., 1989. Flow past short circular cylinders with two free ends. J. Fluid Mech. 203, 557–575.